Ultrabright Fluorescent Silica Mesoporous Silica Nanoparticles: Control of Particle Size and Dye Loading

ARTICLE *in* ADVANCED FUNCTIONAL MATERIALS · AUGUST 2011

Impact Factor: 11.81 · DOI: 10.1002/adfm.201100311

3 AUTHORS:

Eun-Bum Cho
Seoul National University of Science and Te…
36 PUBLICATIONS **482** CITATIONS
SEE PROFILE

Dmytro Volkov
Tyndall Air Force Research Laboratory
12 PUBLICATIONS **176** CITATIONS
SEE PROFILE

Igor Sokolov
Tufts University
179 PUBLICATIONS **3,446** CITATIONS
SEE PROFILE

ADVANCED FUNCTIONAL MATERIALS
www.afm-journal.de

Ultrabright Fluorescent Silica Mesoporous Silica Nanoparticles: Control of Particle Size and Dye Loading

*Eun-Bum Cho, Dmytro O. Volkov, and Igor Sokolov**

The synthesis of ultrabright fluorescent mesoporous silica nanoparticles (UFSNPs) of various sizes loaded with different amounts of fluorescent dye (Rhodamine 6G) is reported here. The dye is physically entrapped inside the nanochannels of the silica matrix created during templated sol–gel self assembly. Due to the specific nanoenvironment, the fluorescence of the encapsulated dye molecules remains unquenched up to very high concentrations, which results in relatively high fluorescence. The particle size (ranging from 20–50 nm) and dye loading (0.8–9.3 mg dye per g particles) are controlled by the timing of the synthesis and the concentration of several organotriethoxysilanes, which are coprecursors of silica. The quantum yields of the encapsulated dye range from 0.65 to 1.0. The relative brightness of a single particle is equivalent to the fluorescence of 30–770 free nondimerized R6G dye molecules in water, or to that of 1.5–39 CdSe/ZnS quantum dots. Despite the presence of some hydrophobic groups on the particles' surfaces, colloidal suspensions of the particles are relatively stable (as monitored for 120 days).

1. Introduction

Fluorescent particles are used in a broad range of applications that involve tagging, tracing, and labeling.[1–5] A myriad of organic (dyes, pigments) and inorganic (dyes, pigments, quantum dots) fluorescent materials have been developed. Fluorescence of colloidal particles is typically achieved by incorporating either inorganic or organic fluorescent materials into the particles' matrix.

Inorganic dyes are typically more stable against oxidation and photobleaching. However, their limited variety, relatively low quantum yields, and limited compatibility restrict their broad utilization. For example, quantum dots,[6] which are the brightest colloidal particles synthesized so far, are not as stable as organic dyes in aqueous environments, have blinking problems, and can be rather toxic when labeling biological objects.[7] The large variety of organic dyes, their high quantum yields, their absence of blinking, their excellent aqueous stability, and their relatively low toxicity make them attractive for use in fluorescent particles. The main problem associated with organic dyes is their relatively fast photobleaching. Some dyes can interfere with some biological processes. Sealing organic dyes into a silica matrix seems to be one of most promising approaches because of the wide compatibility of silica with other—including biological—materials. The chemistry of silica is well known.[8] Hence, it is plausible to expect straightforward functionalization of fluorescent silica particles with various sensing molecules to give the particles preference for adhering to specific molecules or materials.

Various attempts to embed organic dyes into silica xerogels and zeolites have been reported.[9–18] To prevent the dyes leaking out of the porous matrix, dyes have been covalently bound to the silica matrix.[12,14,19–24] One of the costs of such a strong bond is typically a decrease in quantum yield, and hence reduced fluorescent brightness of the material. Nevertheless, nanoparticles as bright as quantum dots have been synthesized by utilizing the covalent attachment of specific dyes to an organosilica matrix.[16,18,25] It has recently been reported that even a physical (i.e., weak) encapsulation inside a nano(or meso)porous silica matrix preserves the quantum yield of the dye.[26,27] The dye was encapsulated through templated sol–gel self assembly of mesoporous particles with fluorescent dye added in relatively large concentration (up to 0.01 M) to the synthesizing bath. The dye molecules became physically entrapped inside nanochannels of 2–4 nm diameter during the synthesis. The synthesized particles were found to be up to two orders of magnitude brighter than the micrometer-size particles assembled from water-dispersible quantum dots encapsulated in polymeric particles (scaled to the same size).[28] The particles showed fluorescence that was higher by a factor of several thousand than the maximum fluorescence of free dye in the same volume.

Ultrabright fluorescent silica nanoparticles (UFSNP) are of broad interest. Increased brightness of labeled silica particles is desirable for attaining a higher signal-to-noise ratio, and consequently, to increase the sensitivity and/or speed of detection. Previously synthesized particles were on the micrometer scale,[26,27]

Dr. E.-B. Cho,[+] Dr. D. O. Volkov, Prof. I. Sokolov
Department of Physics
Clarkson University
8 Clarkson Ave., Potsdam, NY 13699–5820, USA
E-mail: isokolov@clarkson.edu
Prof. I. Sokolov
Department of Chemical and Biomolecular Sciences
and Nanoengineering and Biotechnology Laboratories Center (NABLAB)
Clarkson University
8 Clarkson Ave., Potsdam, NY 13699–5820.
[+] Present address: Department of Fine Chemistry
Seoul National University of Science and Technology
138 Gongreung-Gil, Nowon-Gu, Seoul 139-743, Korea

DOI: 10.1002/adfm.201100311

and there has been a subsequent effort to scale it down to the nanoscale, in order to produce UFSNP.[29] The fluorescence of the dye inside these particles was not quenched, even though its concentration was ≈230 times higher than the maximum nonquenching concentration of free dye in aqueous solution. Nonetheless, these UFSNP were not quite ultrabright. Compared to a popular class of bright fluorescent particles (water dispersible quantum dots)[30] UFSNP have been reported[29] at ≈40% of the quantum dot brightness. This is almost two orders of magnitude lower than that expected from simply geometrically scaling down the previously reported ultrabright micrometer-sized particles,[26,27] which is presumably due to dye leakage from the channels. To prevent this, the channels need to be self sealed by bending, as was the case for the micrometer-sized particles. However, this is thermodynamically impossible.[31] It would require impractically high levels of thermal energy to bend the nanochannels of such small particles.

Here we report the syntheses of UFSNP by using Rhodamine 6G (R6G) fluorescent dye, which has a brightness density (brightness per unit volume) comparable to the reported ultrabright fluorescent micrometer-sized silica particles.[26,27] The dye loading inside UFSNP can be as high as 0.01 g dye per g particles. The particle size (ranging from 20 to 50 nm) and dye loading were controlled through the timing of the synthesis and the concentration of organosilanes (triethoxysilanes), which were used as coprecursors of silica. The use of triethoxysilanes as coprecursors prevents dye leakage,[32] presumably due to the presence of hydrophobic groups, which would help to prevent water from entering the particles, and hence prevent diffusion of the dye molecules out of the particles. Despite the presence of a number of hydrophobic groups on the particles' surfaces, colloidal suspensions of most nanoparticles were quite stable (as monitored for four months).

2. Results and Discussion

The UFSNP were prepared with triethanolamine (TEA) additive and R6G fluorescent dye in a general tetraethyl orthosilicate–cationic surfactant (TEOS–CTA^+) system.[32] UFSNP were synthesized with several different organosilane coprecursors of silica, such as methyltrimethoxysilane (MTMS), ethyltriethoxysilane (ETES), and phenyltriethoxysilane (PTES) (see **Scheme 1**), using two different addition methods (i.e., co-condensation and sequential-grafting methods). The main variation of parameters related to the organosilanes, while other experimental conditions (such as temperature and amount of TEA and water) were fixed.

Table 1. Sample nomenclature and corresponding compositions of reagents used to synthesize fluorescent mesoporous silica nanoparticles by co-condensation and sequential grafting.

Sample	Additional OS[a)]	[OS] × 100/ [total silanes] [mol%]	t_{ad}[b)] [min]	[R6G] [M]
TM10	MTMS	10	0	5×10^{-3}
TM191	MTMS	5	30	5×10^{-3}
TM91	MTMS	10	30	5×10^{-3}
TM571	MTMS	15	30	5×10^{-3}
TM91_60	MTMS	10	60	5×10^{-3}
TE91	ETES	10	30	5×10^{-3}
TP191	PTES	5	30	5×10^{-3}
TP91	PTES	10	30	5×10^{-3}
TP571	PTES	15	30	5×10^{-3}

[a)]OS = organosilane coprecursor materials; [b)]t_{ad} = the time lag before organosilane addition.

The preparation of the UFSNP was based on the synthesis of mesoporous silica nanoparticles, using a TEA (initial pH ≈ 10 and p*K*a = 7.8) additive as a weak base. TEA is known to act as a pH stabilizer and also a sterically bulky chelating material, which is important for controlling the particle diameter.[33] Organosilanes (OS) such as MTMS, ETES, and PTES were used as a cosource of silica, and were added 0, 30, and 60 min after the main silica precursor, TEOS. All samples prepared in this study, along with the chemical composition of each preparation that resulted in particle diameters of <100 nm, are listed in **Table 1**. Other experimental conditions, such as the amount of TEA and water, remained constant for all samples.

2.1 Particle Sizes

To demonstrate mesoscale porosity in the synthesized UFSNP, transmission electron microscopy (TEM) was carried out. **Figure 1** presents the TEM images of several UFSNP prepared in this study; two images of larger and two images of smaller particles are shown. The mesoporous structure of these slightly nonspherical particles can clearly be seen.

The present work is focused on the synthesis of particles with relatively long-term stability. We study the effect of three organosilanes and the synthesis kinetics on the particles' diameter, colloidal stability, and brightness. The long-term stability of the UFSNP diameter and the particles' colloidal suspension were measured by means of dynamic light scattering (DLS).

Table 2 summarizes the DLS results for the synthesized UFSNP. Two types of particle diameter are listed: the most probable diameter (D_m) and the effective diameter (D_{eff}).

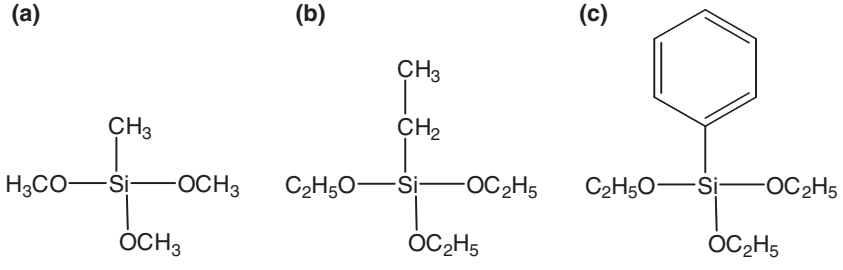

Scheme 1. Molecular structures of organosilanes used in this study; a) MTMS, b) ETES, and c) PTES.

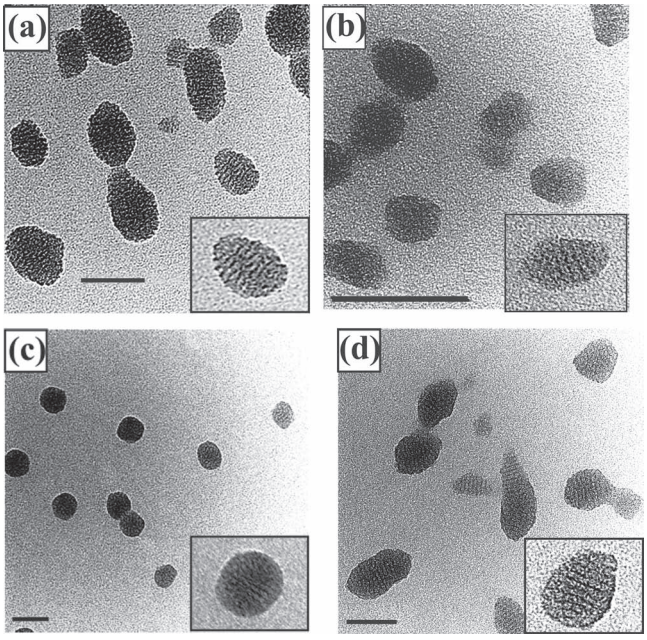

Figure 1. Representative TEM images for several fluorescent mesoporous silica nanoparticles. The images and the corresponding samples are listed in Table 1 as a) TM91, b) TM571, c) TP91, and d) TE91. The insets show enlarged particles. The scale bars are 50 nm.

The most probable diameter represents the size of the most abundant particles in the suspension. The effective diameter, defined by the diffusion coefficient, was found from the analysis of the self-correlation function of intensities (number of photons) of the laser light scattered by the particles. The effective diameter can be taken as average because the entire population of particles defines the scattered light. The polydispersity shown in Table 2 refers to the distribution of the most probable diameter. The difference between the most probable and effective diameters can be explained by multimodal size distributions of the particle sizes, which presumably occurs due to agglomeration of smaller particles into larger aggregates. Even a small number of larger aggregates can substantially shift the average diameter towards larger values.

It can be seen from Table 1 and Table 2 that, typically, 10 mol% secondary organosilane precursors show the lowest effective diameters for samples prepared by sequential grafting (TM91, TM91_60, TE91, TP91). The most probable diameter D_m is smallest for 15% MTMS (sample TM571), 10 mol% of PTES (sample TE91), and 5% of PTES (TP191). One can also see that 30 min is the most effective time lag for decreasing particle diameter.

Table 2. Dynamic light scattering results for UFSNP using co-condensation and sequential grafting.

Sample	D_m[a)] [nm]	D_{eff}[b)] [nm]	Polydispersity
TM10	53	205	0.21
TM191	36	150	0.20
TM91	40	106	0.22
TM571	23	140	0.20
TM91_60	30	92	0.12
TE91	52	88	0.19
TP191	28	120	0.20
TP91	45	78	0.15
TP571	34	140	0.15

[a)] D_m = most probable diameter obtained from the multimodal size distribution results of dynamic light scattering device used in this study; [b)] D_{eff} = effective diameter.

2.2 Stability of Colloidal Suspensions of UFSNP

Colloidal stability was monitored both visually and by using DSL. In the latter case, one can measure the stability of the suspension as well as the stability of the most probable diameter of the particles by monitoring the difference between the most probable and effective diameters (as described in the previous section).

Stability depends on particle concentration. The working concentrations of the as-synthesized suspensions were used, which were relatively high (giving an opaque solution). Visual monitoring showed formation of precipitates within one week (not shown). The supernatant of the colloidal suspension of UFSNP was relatively stable for much longer (several weeks). However, analysis of the zeta potential (see later) indicated that the suspension cannot be stable in the long term.

To perform DLS, UFSNP suspensions extracted by dialysis for one week were diluted by a factor of ten with deionized (DI) water, and filtered using a 200-nm membrane filter to remove any agglomerates. The filtered UFSNP dispersions were kept in quiescent conditions while DLS was measured for up to 120 days. **Figure 2** shows two representative examples of monitoring the effective diameters. As an example, the corresponding initial concentrations of UFSNP were 1.14×10^{-3} g mL^{-1} (TM91) and 2.81×10^{-3} g mL^{-1} (TP91). TP91 represents the most stable sample; its effective diameter remains constant for the entire duration of 120 days. TM91 represents a less stable suspension. One can see a gradual increase of the effective diameter to more than 0.5 micrometer over 50 days. The observed decrease of the effective diameter after 50 days can be explained by precipitation of agglomerates that have grown too large and ceased to undergo Brownian motion (our measurements were performed by sampling of the supernatant part of the suspension; i.e., without particle resuspension. A small amount of precipitant was visible).

The zeta potential can provide information on the interaction of UFSNP with other materials, surfaces, and particles, and is helpful in estimating the colloidal stability of UFSNP suspensions. The higher the zeta potential, the stronger the electrostatic repulsion between the particles. In our system, however, the observed stability was surprisingly not well correlated with the zeta potential of TP91 (11 ± 1 mV) and TM91 (15 ± 2 mV). There are two possible reasons for this: firstly, TM91 particles may possess more attractive groups (either hydrophobic or through the hydrogen interaction) than TP91; or secondly, the distribution of charges may be highly heterogeneous, in which case the particles could easily undergo rotation to minimize

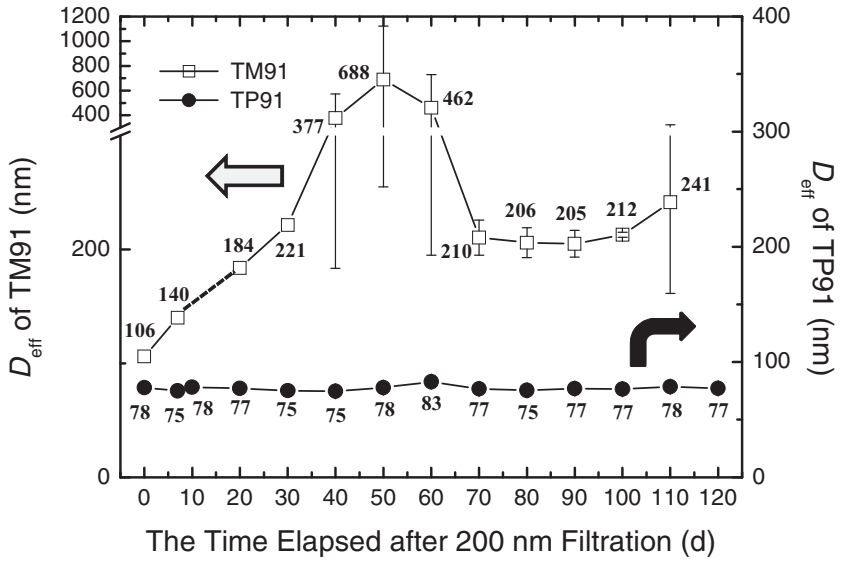

Figure 2. A representative example of DLS data for the effective diameter of UFSNP as a function of time elapsed after 200 nm filtration.

repulsion. This phenomenon is somewhat similar to that reported previously,[34] where the interaction between nanoparticles was found to be substantially different from the interaction between micrometer-sized particles made of the same material; this could not be explained by zeta potential alone. This phenomenon will be studied in detail in future work.

While the stability of the colloidal suspension cannot be explained in terms of zeta potential alone, the zeta potential does define the kinetics of agglomeration. The zeta potentials for our samples ranged between 5 and 20 mV. This is generally considered to be insufficient for long-term stability of colloidal suspensions. At the same time, the stability of individual particles (hydrothermal stability) seems to be high because the most probable diameter of the particles in the supernatant does not change with time.

2.3 Fluorescent Properties of UFSNP

The brightness of the synthesized UFSNP was evaluated after dialysis for one week in DI water. To measure the brightness of a single particle, the fluorescence brightness (the integral of the fluorescent spectrum) of each particle—measured directly using the fluorescent spectrometer—can be deduced from the fluorescent brightness of the spectrum emitted by a single R6G molecule measured with the same spectrometer. Assuming linear dependence of the fluorescent brightness on the quantity of suspended particles (and the dye molecules dissolved in water) used to measure the brightness, one can arrive at the following equation:

$$\text{UFSNPrelativebrightness} = \frac{FL_{\text{UFSNP}}/C_{\text{UFSNP}}}{FL_{\text{R6G}}/C_{\text{R6G}}} \quad (1)$$

where $FL_{\text{UFSNP}}/C_{\text{R6G}}$ is the (integral) amount of fluorescent light coming from a suspension of UFSNP in water (solution of R6G dye), and $C_{\text{UFSNP}}/C_{\text{R6G}}$ is the density of UFSNP (dye concentration) in the measured suspension (solution).

The assumption of linearity used in Equation (1) is only correct for sufficiently small concentrations of suspended particles (dissolved dye molecules in water). Therefore, special care was taken to ensure that the measurements were performed in the linear regime. This was verified by sequential dilution of the analyte, and by monitoring the corresponding decrease in the brightness. Note that this approach takes into account the partial scattering of the excitation light by UFSNP. To find the UFSNP relative brightness, we typically measured the amount of fluorescence coming from 10 μL of a UFSNP stock suspension diluted to 3 mL with water. For example, the integral fluorescence of TM91 was FL_{UFSNP} 8610 au (the error in the fluorescence measurement was negligible). To find C_{UFSNP}, the stock suspension was weighed with a quartz microbalance (QCM) and also with a high-resolution balance. In the case of TM91, the average was (1.14 ± 0.15) mg particles per mL water. Taking the known density of the nanoporous silica material (1.6 g cm^{-3} [27,35]), and the most abundant diameter of TM91 UFSNP (40 nm), the density of nanoparticles in the measured suspension was $C_{\text{FMSNP}} = (7.1 \pm 0.9) \times 10^{10}$ particles per mL water. Similarly, the brightness of a single molecule of R6G dye was determined; $FL_{\text{R6G}} = 7635$ au was found from the dye concentration $(7.0 \pm 0.5) \times 10^{-8}$ M (from the Beer–Lambert law), or $C_{\text{R6G}} = (4.2 \pm 0.3) \times 10^{13}$ dye molecules per mL water. Thus, from Equation (1), the UFSNP fluorescent brightness of TM91 is equivalent to the brightness of approximately 670 molecules of free nondimerized R6G dissolved in water. This can be further related to the brightness of, for example, a single ZnS-capped CdSe quantum dot (which is ≈20 times brighter than a molecule of R6G[36,37]). Thus the brightness of TM91 UFSNP is 34 × higher than a single ZnS-capped CdSe quantum dot. Moreover, the UFSNP seem to be substantially brighter than that of previously reported fluorescent silica nanoparticles,[16,20,38–43] in which the brightness of the reported particles was equivalent to the fluorescence of one quantum dot.

The quantum yield (QY) was calculated by using the standard formula shown in Equation (2)

$$QY = 95\% \frac{FL_{\text{UFSNP}}}{A_{\text{R6G of UFSNP}}} \frac{A_{\text{R6G}}}{FL_{\text{R6G}}} \quad (2)$$

where $A_{\text{R6G of UFSNP}}$ (A_{R6G}) is the absorbance of the R6G dye extracted from UFSNP (concentration of R6G reference dye, which should be quite low to avoid the nonlinear effects mentioned above; here we used ≈10^{-7} M). The quantum yield of R6G reference dye is 95%. $A_{\text{R6G of UFSNP}}$ was found as follows: A small volume of UFSNP colloidal suspension was dried and weighed as described above. Then, a small volume of the same UFSNP suspension was dissolved using 1% hydrofluoric acid. Note that the extinction coefficient of R6G dye in water remains the same in the presence of 1% hydrofluoric acid (consequently one can use Equation (2)). $A_{\text{R6G of UFSNP}}$ was found by scaling

Table 3 Properties of fluorescent mesoporous silica nanoparticles.

Sample	A[a]	F_{area}[b] [au]	Φ_{UFSNP}[c]	$W_{dye/UFSNP}$[d] [mg g^{-1}]	D_m [nm]	Relative brightness [no. of free R6G molecules]
R6G	0.007	7630	0.95	n/a	n/a	1
TM10	0.013	10180	0.69	1.7	53	190
TM191	0.008	7710	0.84	4.6	36	190
TM91	0.0047	8610	1.01	9.3	40	670
TM571	0.013	9640	0.65	7.0	23	58
TM91_60	0.009	7660	0.78	5.7	30	130
TE91	0.0067	7850	1.02	5.1	52	770
TP191	0.005	4590	0.82	2.2	28	43
TP91	0.0098	9980	0.89	2.5	45	211
TP571	0.002	2145	0.98	0.8	34	32

[a] A is the UV absorbance at a wavelength of 525 nm for UFSNP samples treated with HF (1 wt% solution); [b] $F_{area,\ DI\ water}$ is the integrated area of fluorescence emission spectra for UFSNP samples in DI water; [c] Φ_{UFSNP} is the quantum yield calculated using fluorescence emission and UV absorbance based on the R6G 7 × 10^{-8} M standard solution; [d] $W_{dye/UFSNP}$ is the mass of R6G dye encapsulated in 1 g of UFSNP.

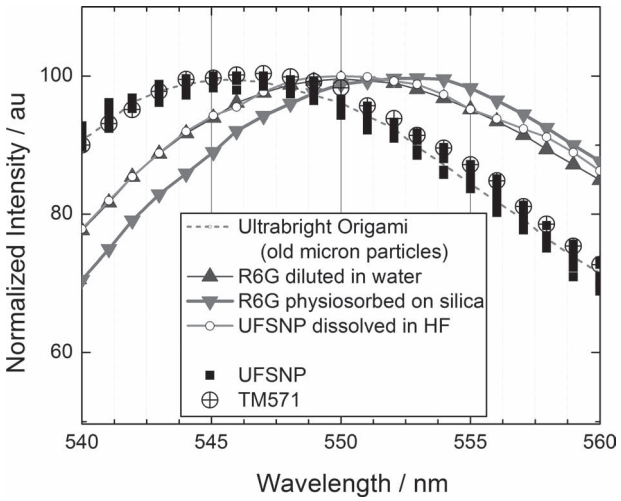

Figure 3. High-resolution fluorescence spectra of UFSNP, ultrabright (origami) micrometer-sized particles,[27] free R6G solution in water (1 μM), UFSNP dissolved in 1% HF solution, and R6G electrostatically physisorbed onto 60 nm solid silica particles.[29] TM571 UFSNP is shown separately as an example of the lowest quantum yield.

up the concentration proportionally for the HF solution. For TM91, for example, we found FL_{FMNSP} = 8610 au, FL_{R6G} = 7635 au, $A_{R6G\ of\ UFSNP}$ = 0.0074 ± 0.0005, and A_{R6G} = 0.0070 ± 0.0005. From Equation (2), QY = 1.0 ± 0.1.

This method also allows us to find the concentration of R6G inside the particles, which was 9.3 mg g^{-1} (9.3 mg dye per g particles) or 31 mM. This is similar to the concentration found in ultrabright micrometer-sized particles[26,27].

Table 3 shows the results of similar measurements on the rest of our samples. The concentration of R6G inside the particles varied from 0.8 to 9.3 mg g^{-1}, while the quantum yield, Φ, of the encapsulated dye varied from 0.65 to 1.02. The particles' brightness varied from 30 to 770 × the brightness of individual free nondimerized R6G dye molecules. This is also equivalent to the brightness of 1.5–39 CdSe/ZnS quantum dots.

The above calculations were based on the assumption that no free dye had leaked into the solution used to measure the fluorescence, which would affect both brightness and quantum yield. Thus, it is important to test for the presence of leaked dye by examining the high-resolution fluorescence spectrum near its maximum and monitoring the stability of the peak positions. As shown in **Figure 3**, the aqueous solution of free dye shows a fluorescence maximum at 550 nm (solid curve). At the same time, the fluorescence of the dye encapsulated inside of the particles displays a characteristic blueshift of 5 nm. This can be explained by the nonpolar environment of the nanoporous channels,[29,32] and by a caging effect.[44] These spectra were used to monitor possible leakage of the encapsulated dye.

Note that physical adsorption of R6G dye onto silica particles[29] leads to a significant redshift of the fluorescence maximum relative to the free dye in water, which is also shown in Figure 3. Note also that TM571, which has the lowest quantum yield, also shows a significant redshift relative to other UFSNP. We may speculate that the decrease of quantum yield in this case is caused by the strong physical interaction between R6G dye molecules and the silica matrix of UFSNP (such a decrease has been reported for the interaction between fluorescent dyes and xerogels[11,14]).

Figure 3 has further useful information; after the particles have been dissolved in HF, the spectrum is virtually identical to that of the free dye. This supports our use of the Beer–Lambert law to find the concentration of the dye inside the particles after dissolving in HF.

An important property of the ultrabright particles is that the fluorescence of the encapsulated dye inside the particles is not quenched, despite a relatively high concentration of the encapsulated dye. The maximum concentration inside the particles is >5000 × higher than the concentration of R6G dye in water at which there is no noticeable dimerization/homoquenching (dimerization happens before fluorescence quenching in the case of R6G dye). The absence of dimerization can be verified by recording the fluorescence spectra of the particles excited by various wavelengths. **Figure 4** shows several examples of such spectra corresponding to TM91/TE91/TP571 (identical spectra), TM571 (lowest quantum yield), free R6G dye in water with and without dimerization/fluorescent quenching. The particles with high quantum yields do not show any changes in the spectra specific for dimerization of R6G dye molecules. Interestingly, there is virtually no noticeable dimerization/spectral broadening even in the case of TM571, which has a low quantum yield. This implies that the decrease in quantum yield for UFSNP reported here is largely due to the interaction between the dye molecules and the silica matrix (as discussed above), rather than from self quenching of the dye.

3. Conclusion

Fluorescent mesoporous silica nanoparticles synthesized in the presence of a small amount of secondary silica coprecursor organosilanes (MTMS, ETES, or PTES) were prepared by using

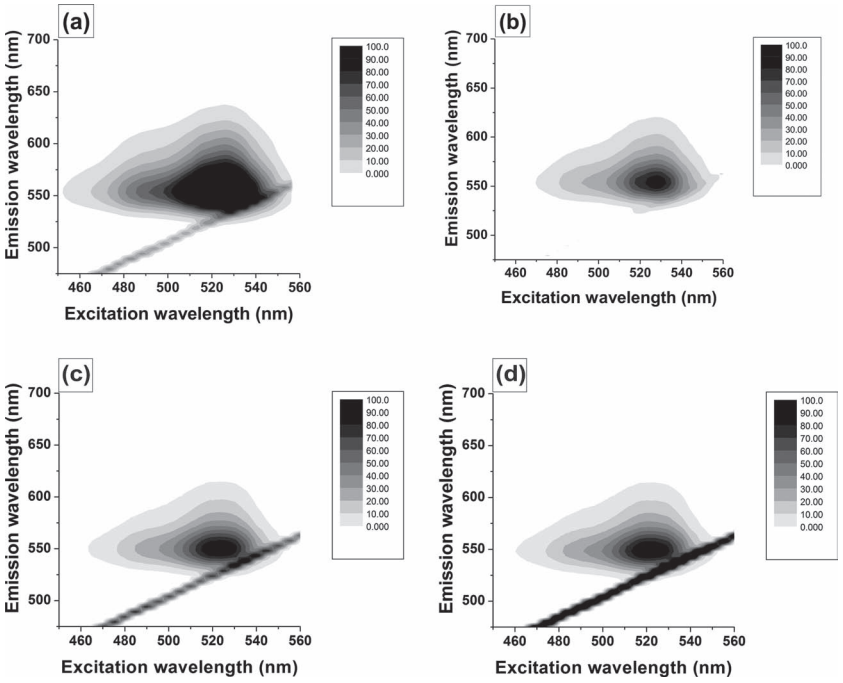

Figure 4. Examples of fluorescence spectra of UFSNP excited at various wavelengths. (a) Free R6G dye in water demonstrating dimerization ([dye] $\approx 1 \times 10^{-5}$ M); (b) Free R6G dye in water demonstrating virtually no dimerization ([dye] $\approx 3 \times 10^{-7}$ M); (c) The spectra corresponding to TM91/TE91/TP571 (highest quantum yield). The spectra of these three samples are identical within the error of measurement; (d) TM571 (lowest quantum yield).

co-condensation (with no time lag) and sequential grafting (with time lags of 30 or 60 min) methods. The most abundant diameter of the UFSNP was ≤50 nm. R6G was used as the organic fluorescent dye, while triethanolamine was utilized as a pH stabilizer and a bulky chelating material to attain nanoscale diameters of UFSNP samples. Organosilane–UFSNP prepared in this study showed a size range of 20–50 nm (most probable diameter from DLS measurements). The fluorescent brightness of single particles was reported relative to the fluorescent brightness of a single free nondimerized R6G dye molecule in water. The brightness of single UFSNP were in the range of 30–770 R6G dye-molecule brightness. This is equivalent to the brightness of 1.5–39 CdSe/ZnS quantum dots. The particles were relatively stable for the monitored period of 120 days. No leakage of the dye out of the silica matrix of the particles was found. At the same time, the colloidal stability of the particles was reasonable but not particularly high (except for one PTES–UFSNP sample, which was more stable).

4. Experimental Section

Chemicals: TEOS, MTMS, ETES, and PTES (Aldrich) were used as silica sources. Cetyltrimethylammonium chloride (CTAC, 25% aqueous solution, Aldrich) was used as a structure-directing agent, and TEA (Aldrich) as an additive. R6G (Exciton) was used as a fluorescent dye. All chemicals were used without further purification. Ultrapure DI water from a Mili-Q ultrapure system was used for all synthesis, dialysis, and storage steps.

Preparation of Fluorescent Mesoporous Nanoparticles by Co-Condensation with MTMS: The synthesis was based on the use of TEA as a replacement for NaOH catalyst.[23] The relative molar composition of 1.0 total silanes was 0.2 CTAC: 0.02–0.04 R6G: 10.4 TEA: 141.6 H_2O. In a typical synthesis of UFSNP TEOS, MTMS, and TEA were combined and heated for 1 h at 90 °C without stirring. An aqueous solution of R6G and CTAC was stirred at 60 °C for 1 h. The two solutions were then combined and stirred for 5 h.

Preparation of Fluorescent Mesoporous Nanoparticles by Sequential Grafting with Organosilane: In a typical synthesis of UFSNP, TEOS, and TEA were combined and heated for 1 h at 90 °C without stirring. An aqueous solution of R6G and CTAC was stirred at 60 °C for 1 h. The two solutions were then combined and stirred at room temperature for 30 min before the PTES coprecursor was added and the solution stirred for a further 4.5 h at room temperature.

General Extraction Method of UFSNP: Any remaining reactants (CTAC, TEA, residual silica precursors, and R6G dye) were removed from the UFSNP products using dialysis. About 40 g of UFSNP solution product was dialyzed with DI water using a Spectra/Por® RC membrane, MW ≈ 10–15 kDa membrane until the supernatant water showed no fluorescence (up to several days).

Preparation of Particle Suspension for Stability Test and DLS: Following dialysis, UFSNP were diluted 10 × before filtering with a 200 nm membrane to remove possible agglomerations. The size distribution of UFSNP was measured by using DLS at various times after filtration. Both effective and most probable diameters were recorded.

Characterization: DLS and zeta-potential measurements of UFSNP were performed with a particle-size analyzer (Brookhaven, NY) equipped with a standard 35 mW diode laser and an avalanche photodiode detector. To determine the diameter, 50 µL of a stock solution of UFSNP was mixed with 3 mL of distilled water in a polystyrene cuvette. Each sample was scanned for 9 min (3 runs) to obtain one set of raw data for the effective and most probable diameters. Both diameters of UFSNP were found using 90Plus particle-sizing software. Average values were determined with at least three measurements per sample. Zeta potentials of UFSNP were obtained using ZetaPALS software. 30 µL of the extracted sample was mixed with 1.5 mL of distilled water. Average values for the zeta potential were determined with at least three measurements with 10 runs per sample.

TEM images were obtained with a high-resolution JEM2010 (JEOL, Japan) scanning TEM microscope (200 kV accelerating voltage) equipped with a LaB_6 cathode and a Gatan SC1000 CCD camera. For TEM measurements, an adequate amount of extracted UFSNP was dropped onto a porous carbon film on a copper grid and then dried in vacuum.

A fluorescence spectrophotometer (Varian, Cary Eclipse), and a UV-2401PC UV–vis spectrophotometer (Shimadzu, Japan) were used to measure the fluorescence of UFSNP and concentration of R6G dye inside UFSNP. Samples were prepared under the same conditions as those used for DLS, while 1 wt% HF solution was used to obtain the concentration of R6G dye extracted from UFSNP.

Weighing by Means of QCM: A suspension of UFSNP in water (5 µL) was dried on the surface of a QCM (QCM922, Princeton Applied Research, TN, USA). The mass of the UFSNP was found from the change in resonance frequency of the quartz crystal. While QCM is a standard method, there is a danger of artifacts when measuring large samples of nanoparticles (due to a possible damping of QCM vibrations in loosely attached nanoparticles). The absence of this artifact was verified by sequential dilution of the UFSNP suspension, and its subsequent reweighing with QCM.

Weighing by Means of High-Resolution Balance: A suspension of UFSNP in water (0.1–0.7 mL) in an aluminum foil cap was dried in a vacuum chamber for 24 hours. Weighing was performed five times on a CAHN29 balance (CAHN Instruments; sensitivity 0.1 μg).

Acknowledgements

I.S. acknowledges partial support of this work by the National Science Foundation (CBET 0755704) and the Army Research Office (W911NF-05–1–0339).

Received: February 9, 2011
Published online: June 7, 2011

[1] U. Hasegawa, S. I. Nomura, S. C. Kaul, T. Hirano, K. Akiyoshi, *Biochem. Biophys. Res. Commun.* **2005**, *331*, 917.
[2] B. S. Edwards, T. Oprea, E. R. Prossnitz, L. A. Sklar, *Curr. Opin. Chem. Biol.* **2004**, *8*, 392.
[3] G. Lizard, S. Monier, C. Prunet, L. Duvillard, P. Gambert, *Ann. Biol. Clin. (Paris)* **2004**, *62*, 47.
[4] R. M. Gaikwad, M. E. Dokukin, K. S. Iyer, C. D. Woodworth, D. O. Volkov, I. Sokolov, *Analyst* **2011**, *136*, 1502.
[5] S. Iyer, C. D. Woodworth, R. M. Gaikwad, Y. Y. Kievsky, I. Sokolov, *Small* **2009**, *5*, 2277.
[6] U. Resch-Genger, M. Grabolle, S. Cavaliere-Jaricot, R. Nitschke, T. Nann, *Nat. Methods* **2008**, *5*, 763.
[7] R. Hardman, *Environ. Health Perspect.* **2006**, *114*, 165.
[8] R. K. Iler, *The Chemistry of Silica: Solubility, Polymerization, Colloid and Surface Properties and Biochemistry of Silica* Wiley-Interscience, **1979**.
[9] A. P. Rao, A. V. Rao, *Mater. Lett.* **2003**, *57*, 3741.
[10] A. M. Klonkowski, K. Kledzik, R. Ostaszewski, T. Widernik, *Colloid Surf. A* **2002**, *208*, 115.
[11] A. V. Deshpande, U. Kumar, *J. Non-Cryst. Solids* **2002**, *306*, 149.
[12] N. Leventis, I. A. Elder, D. R. Rolison, M. L. Anderson, C. I. Merzbacher, *Chem. Mater.* **1999**, *11*, 2837.
[13] F. del Monte, D. Levy, *J. Phys. Chem. B* **1998**, *102*, 8036.
[14] T. Suratwala, Z. Gardlund, K. Davidson, D. R. Uhlmann, J. Watson, N. Peyghambarian, *Chem. Mater.* **1998**, *10*, 190.
[15] G. Calzaferri, S. Huber, H. Maas, C. Minkowski, *Angew. Chem. Int. Ed.* **2003**, *42*, 3732.
[16] X. J. Zhao, R. P. Bagwe, W. H. Tan, *Adv. Mater.* **2004**, *16*, 173.
[17] S. Santra, J. Xu, K. Wang, W. Tan, *J. Nanosci. Nanotechnol.* **2004**, *4*, 590.
[18] Z. Yang, X. S. Kou, W. H. Ni, Z. H. Sun, L. Li, J. F. Wang, *Chem. Mater.* **2007**, *19*, 6222.
[19] P. Audebert, F. Bresson, R. Devillers, G. Tribillon, *Synthetic Met* **1996**, *81*, 315.
[20] R. P. Bagwe, C. Y. Yang, L. R. Hilliard, W. H. Tan, *Langmuir* **2004**, *20*, 8336.
[21] R. Frantz, C. Carbonneau, M. Granier, J. O. Durand, G. F. Lanneau, R. J. P. Corriu, *Tetrahedron Lett.* **2002**, *43*, 6569.
[22] G. A. Baker, S. Pandey, E. P. Maziarz, F. V. Bright, *J. Sol–Gel Sci. Technol.* **1999**, *15*, 37.
[23] Y. S. Lin, C. P. Tsai, H. Y. Huang, C. T. Kuo, Y. Hung, D. M. Huang, Y. C. Chen, C. Y. Mou, *Chem. Mater.* **2005**, *17*, 4570.
[24] J. M. Antonini, D. R. Hemenway, G. S. Davis, *Exp. Lung Res.* **2000**, *26*, 71.
[25] H. Ow, D. R. Larson, M. Srivastava, B. A. Baird, W. W. Webb, U. Wiesner, *Nano Lett.* **2005**, *5*, 113.
[26] S. P. Naik, I. Sokolov, in *Nanoparticles: Synthesis, Stabilization, Passivation and Functionalization*, (Ed: R. Nagarajan), ACS, **2008**, 214.
[27] I. Sokolov, Y. Kievsky, J. M. Kaszpurenko, *Small* **2007**, *3*, 419.
[28] M. Y. Han, X. H. Gao, J. Z. Su, S. Nie, *Nat. Biotechnol.* **2001**, *19*, 631.
[29] I. Sokolov, S. Naik, *Small* **2008**, *4*, 934.
[30] I. L. Medintz, H. T. Uyeda, E. R. Goldman, H. Mattoussi, *Nat. Mater.* **2005**, *4*, 435.
[31] D. O. Volkov, J. Benson, Y. Y. Kievsky, I. Sokolov, *Phys. Chem. Chem. Phys.* **2010**, *12*, 341.
[32] E. B. Cho, D. O. Volkov, I. Sokolov, *Small* **2010**, *6*, 2314.
[33] J. Kecht, A. Schlossbauer, T. Bein, *Chem. Mater.* **2008**, *20*, 7207.
[34] Q. K. Ong, I. Sokolov, *J. Colloid Interface Sci.* **2007**, *310*, 385.
[35] K. J. Edler, P. A. Reynolds, J. W. Whitea, D. Cookson, *J. Chem. Soc., Faraday Trans.* **1997**, *93*, 199.
[36] W. C. W. Chan, D. J. Maxwell, X. H. Gao, R. E. Bailey, M. Y. Han, S. M. Nie, *Current Opinion Biotechnol.* **2002**, *13*, 40.
[37] W. C. W. Chan, S. M. Nie, *Science* **1998**, *281*, 2016.
[38] S. Shibata, T. Taniguchi, T. Yano, M. Yamane, *J. Sol–Gel Sci. Technol.* **1997**, *10*, 263.
[39] H. Ow, D. R. Larson, M. Srivastava, B. A. Baird, W. W. Webb, U. Wiesner, *Nano Lett.* **2005**, *5*, 113.
[40] D. R. Larson, A. Heikal, H. Ow, M. Srivastava, U. Wiesner, B. Baird, W. W. Webb, *Biophys. J.* **2003**, *84*, 586a.
[41] L. Wang, W. H. Tan, *Nano Lett.* **2006**, *6*, 84.
[42] H. H. Yang, H. Y. Qu, P. Lin, S. H. Li, M. T. Ding, J. G. Xu, *Analyst* **2003**, *128*, 462.
[43] S. Kim, H. E. Pudavar, P. N. Prasad, *Chem. Commun.* **2006**, 2071.
[44] A. Anedda, C. M. Carbonaro, F. Clemente, R. Corpino, S. Grandi, A. Magistris, P. C. Mustarelli, *J. Non-Cryst. Solids* **2005**, *351*, 1850.